Case Studies in Construction Materials 16 (2022) e01125

Contents lists available at ScienceDirect

Case Studies in Construction Materials

journal homepage: www.elsevier.com/locate/cscm

Short communication

Reinforcing effect of surface-modified steel fibers in ultra-high-performance concrete under tension

Booki Chun, Soonho Kim, Doo-Yeol Yoo *

Department of Architectural Engineering, Hanyang University, 222 Wangsimni-ro, Seongdong-gu, Seoul 04763, Republic of Korea

ARTICLE INFO

Keywords:
Ultra-high-performance fiber-reinforced concrete
Direct tensile behavior
Chemical treatments
Acetone
Nano-silica
Ethylene-diamine-tetraacetic acid

ABSTRACT

The direct tensile behavior of ultra-high-performance surface-modified steel fiber-reinforced concrete was evaluated in this study. Various chemical modifications were applied to steel fibers, including acetone washing, hydrochloric acid washing, zinc phosphating, silica coating, and chelation using an ethylenediaminetetraacetic acid (EDTA) electrolyte solution, which improved the tensile strength, tensile strain, and g-value to a maximum of 17.76 MPa, 1.22%, and 144.51 kJ/m^3, respectively. Acetone washing and EDTA chelating were the most effective methods for improving the tensile strength, whereas silica coating was the best for improving the strain capacity and energy absorption capacity. The optimal treatment time for EDTA chelation treatment was approximately 6 h, and the tensile performance decreased considerably after 12 h of treatment. Comparing these results with those of pullout experiments revealed that a high shear stress should be maintained after the fiber has fully debonded to effectively enhance the post-cracking tensile performance.

1. Introduction

Ultra-high-performance concrete (UHPC) is widely used in modern structures owing to its remarkable strength and durability. Generally, during the mixing procedure, it is supplemented with fibers, which impart several desirable properties to the UHPC. For instance, UHPC containing steel fibers exhibits high tensile strength and ductility and is suitable for application in the informal construction sector. Thus, steel fibers can potentially replace a portion of conventional steel reinforcing bars in UHPC. In addition to research on improving the performance of the matrix by using various novel materials, efforts to further improve the ductility by revising the fiber properties have continued.

Several methods have been devised to modify the steel fiber properties. These properties can be effectively modified by varying the shape [1–3] or size [4–6] of the fiber. Wille and Naaman [3] investigated the different pullout mechanisms of straight and deformed steel fibers within a high-strength cementitious matrix. They used straight, hooked-end, and twisted fibers; the equivalent bond strength of the deformed fibers was four to five times that of the straight fibers embedded in the same matrix. Chun and Yoo [6] measured the fiber bond strength by replacing macrosteel fibers with micro-steel fibers in a pullout experiment. The appropriate replacement ratio to maximize the bond strength was 1.5% (volume fraction, vol%) of the total 2.0 vol%. However, in such cases, considering that the composite behavior cannot be accurately predicted owing to various factors such as fiber orientation and critical matrix volume, the opposite tendency was derived from the results of the pullout test [6,7]. In another method, the roughness of the

* Corresponding author.
E-mail address: dyyoo@hanyang.ac.kr (D.-Y. Yoo).

https://doi.org/10.1016/j.cscm.2022.e01125
Received 18 January 2022; Received in revised form 11 April 2022; Accepted 29 April 2022
Available online 5 May 2022

steel fibers is improved through physical adjustment or chemical treatment of the fiber surface to enhance the bond strength. Stengel [8] and Chun and Yoo [9] roughened the fiber surface with abrasive papers of different grits. However, polishing the fiber surface is not a suitable approach for composites: this method is not feasible for application on a large scale, and the quality may deteriorate.

Thus, in this study, chemical treatment was considered for modifying the fiber surface as it does not affect the fiber orientation and is feasible for mass production. In particular, five different chemical treatment methods have been employed in several studies [10–14]. Fu and Chung [10] washed stainless-steel fibers with acetone and hydrochloric acid and examined their pullout resistance and contact electrical resistivity. Acetone was effective in strengthening the adhesion owing to its cleansing effect, whereas hydrochloric acid generated interfacial voids in the surrounding matrix. In a study, Sugama et al. [11] coated steel fibers with zinc phosphate to determine the anti-corrosion effect of the zinc phosphate coating; according to the results, the coating improved the adhesion of the fibers. Pi et al. [12,13] coated steel fibers with nanosilica particles; these particles increased the density of the surrounding matrix, and the adhesion performance improved significantly owing to participation in the cement hydration process around the fiber. Kim et al. [14] roughened the surface of steel fibers via the chelating effect of an ethylenediaminetetraacetic acid (EDTA) electrolyte solution. As the EDTA captured the ionized ferrite ions, the fibril of the fibers peeled off, and their roughness increased significantly.

The results of this study are in agreement with those reported in a study by Chun et al. [15], who conducted a fiber pullout experiment by adopting the aforementioned chemical treatment methods: the pullout resistance of chemically modified fibers within UHPC improved sufficiently. In addition, because chemical modification can be easily applied to commercially available products without the need for additional processes such as deformation or polishing, it is a viable technique for production in large volumes. Therefore, if satisfactory results are observed in the composite test, as in the pullout test, the tensile performance of UHPC can be greatly improved through this production technique.

In this study, various chemically treated steel fibers were produced as a novel reinforcement material for UHPC, and each fiber was subjected to atomic force microscopy (AFM) image analyses to determine its surface roughness and morphology prior to specimen fabrication. Dog bone-shaped UHPC specimens were fabricated, and their direct tensile strength was tested. Subsequently, tensile parameters, such as the post-cracking strength, strain capacity, and strain energy per unit volume (*g*-value), were investigated and compared with the interfacial shear stress obtained from the results of the single fiber pullout test.

2. Experimental program

2.1. Materials and mix proportion

A limited number of materials were used to fabricate a UHPC mixture with a compressive strength of approximately 200 MPa. Silica fume as the cementitious material and silica flour as the filler were added to ordinary Portland cement to disperse the size of the particles, and similarly, silica sand with a particle size of 0.3 mm or less was used as the fine aggregate. To ensure sufficient fluidity, even at an extremely low water-to-binder ratio of 0.2, a high-performance water-reducing polycarboxylate-type agent was employed. The mixture proportions of all materials and their particle size distributions are listed in Table 1 and Fig. 1, respectively. A uniform type of steel fiber was used in this study (aspect ratio: 100 (30 mm/0.3 mm); density: 7.9 g/mm^3; tensile strength: 2580 MPa; elastic modulus: 200 GPa).

2.2. Chemical treatment process

Fiber bundles were treated in agreement with the treatment process described in a study [15]; these bundles were prepared to correlate the pullout behavior of the fibers subjected to various chemical treatment methods with the behavior within the composite. Because considerable amounts of fibers were prepared to attain a volume fraction of 2%, the required amounts of solutions and chemicals were correspondingly increased to minimize any differences in performance among the fibers used in the single fiber pullout experiment.

Acetone washing [10]: An acetone solution (99.5% by concentration) was prepared; the fibers were immersed in the acetone solution and stirred for 5–10 min. Subsequently, the fibers were removed from the solution and air-dried at laboratory temperature for 10–15 min

Acid washing [10]: A hydrochloric acid solution with a concentration of 35% was prepared; the fibers were immersed in the hydrochloric acid solution and stirred for 5–10 min. Thereafter, the fibers were removed from the solution and rinsed with distilled water. The samples were then dried in an oven at 200 °C for 10 min

Zinc phosphate [11]: Zinc phosphate tetrahydrate, zinc orthophosphate tetrahydrate, and phosphoric acid solution with a

Table 1
Mixture proportion of UHPC.

W/B†	Mix design [kg/m^3]					
	Water	Cement	Silica fume	Silica sand	Silica flour	SP*
0.2	160.3	788.5	197.1	867.4	236.6	52.6

[Note] W/B = water-to-binder ratio and SP = superplasticizer
*Superplasticizer includes 30% solid (= 15.8 kg/m^3) and 70% water (= 36.8 kg/m^3)
†W/B is calculated by dividing total water content (160.3 kg/m^3 + 36.8 kg/m^3) by total amount of binder (788.5 kg/m^3 + 197.1 kg/m^3)

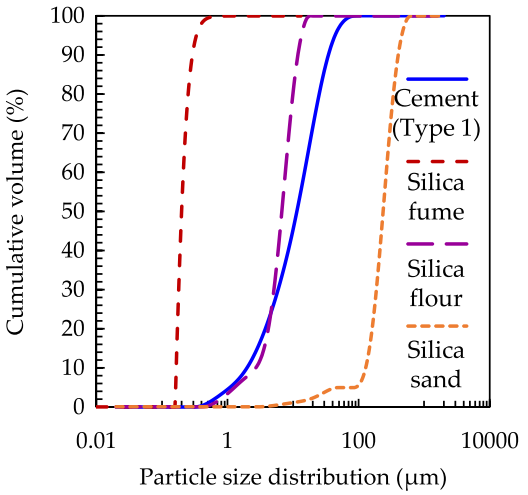

Fig. 1. Particle size distribution.

concentration of 85% were prepared. The chemicals were mixed in the following weight percent ratios: 0.5 wt% zinc orthophosphate tetrahydrate, 0.9 wt% phosphoric acid, and 98.6 wt% distilled water. The ZnPh-convertible solution was heated to 90 °C, and the fibers were immersed in the solution for 5 min. Subsequently, the fibers were removed from the solution and rinsed with distilled water. The samples were finally dried in an oven at 150 ℃ for 10 min

Nanosilica coating [12,13]: Anhydrous ethanol was prepared for use as a solvent, and tetraethyl orthosilicate (TEOS) and cetyltrimethylammonium bromide (CTAB) were obtained as the reaction materials. The chemicals with the following weight percent ratio were mixed: 8.62 wt% TEOS, 0.90 wt% CTAB, and 90.47 wt% anhydrous ethanol. The fibers were immersed in this solution and ultrasonicated for 30 min. Thereafter, 28% concentration of ammonium hydroxide (4 vol% to the solvent) was added to create an alkaline environment. The solution was double-boiled in a 45 ℃ water bath for 12 h. Subsequently, the fibers were removed from the solution and rinsed with distilled water. The samples were then dried in an oven at 80 °C.

EDTA chelation [14]: Sodium carbonate and ethylenediaminetetraacetic acid (EDTA) were prepared beforehand; the chemicals were dissolved in distilled water at molar concentration of 0.1 and 0.045, respectively. The fibers were immersed into the solution for the target periods of 6, 12, and 18 h. The fibers were removed from the solution and rinsed with distilled water; the samples were subsequently stored in anhydrous ethanol to prevent further chemical reactions.

2.3. AFM analysis

AFM was utilized to visualize the surface conditions and evaluate the surface roughness factor, R_q, to better understand the interfacial bond resistance of the plain and chemically treated steel fibers in the UHPC matrix. R_q can be calculated using Eq. (1).

$$R_q = \sqrt{\frac{1}{n}\sum_{i=1}^{n} y_i^2} \tag{1}$$

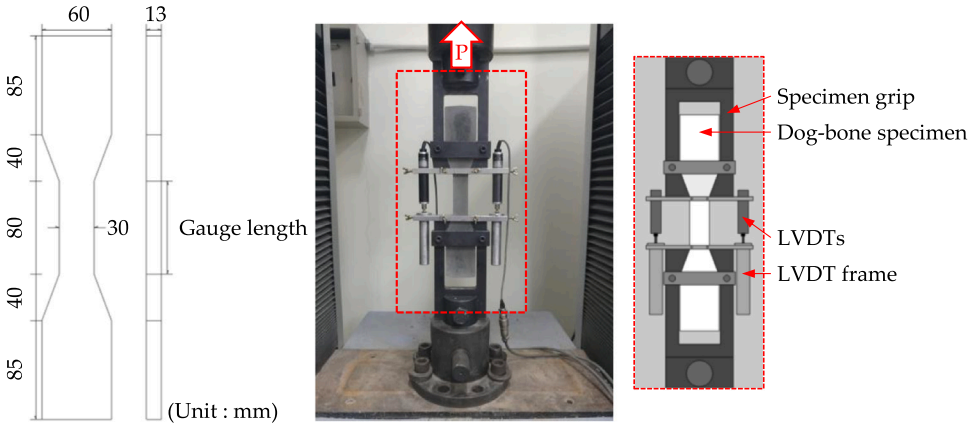

Fig. 2. Direct tensile specimen and test setup.

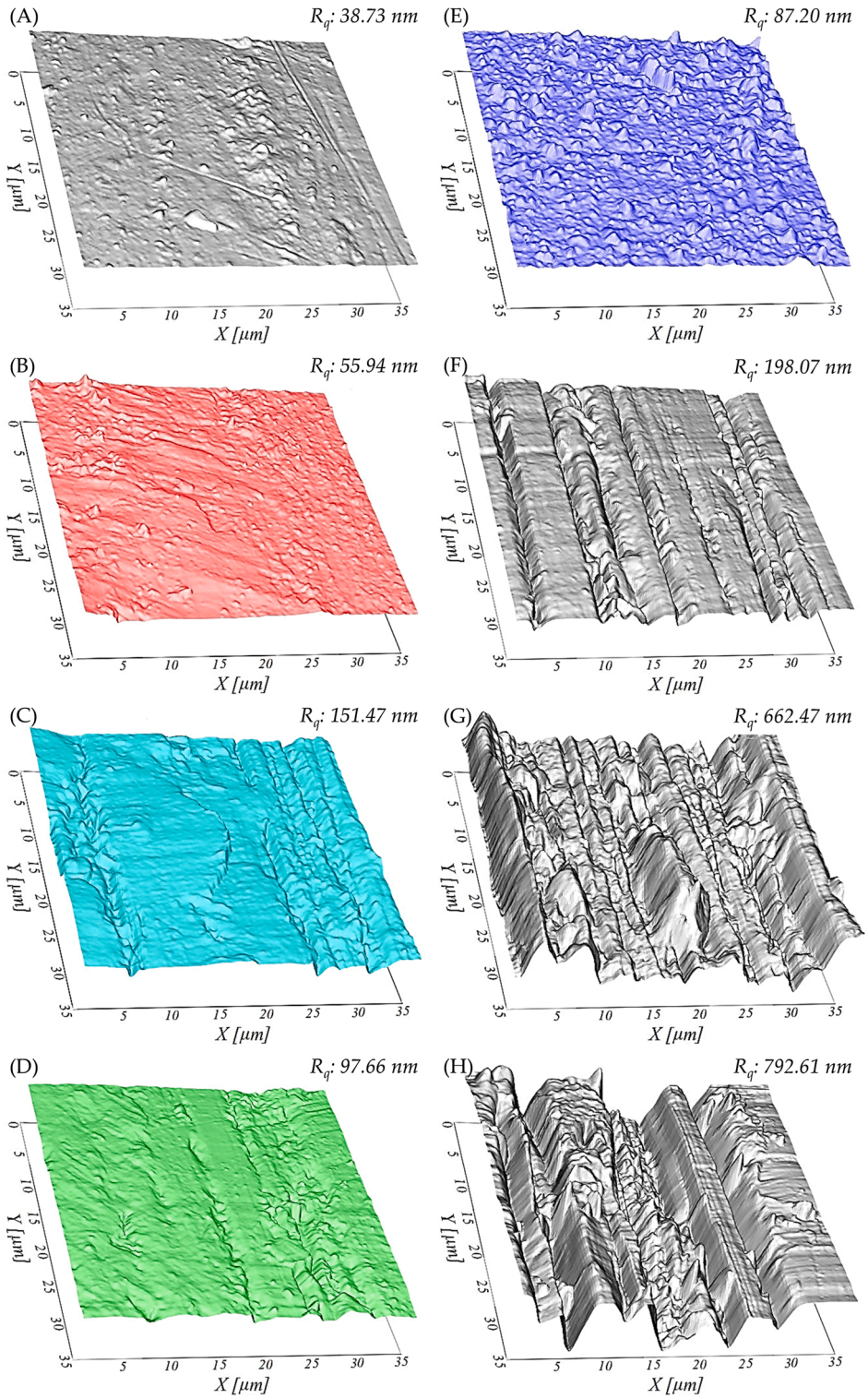

Fig. 3. AFM images and surface roughness of modified steel fiber surface: (A) Plain, (B) Acetone washing, (C) Hydrochloric acid washing, (D) Zinc phosphating, (E) Silica coating, and (F)–(H) EDTA chelating.

where n depicts the number of data points, and y_i symbolizes the height profile of the i^{th} data point.

As demonstrated in a study by Chun et al. [15], a 35 × 35 μm^2 area of the fiber flank was captured via AFM. The height profiles were flattened according to the coordinates during the correction [9]. The corrected data were converted to the root mean squared parameters of the height profiles, R_q, according to the aforementioned equation and imaged by using the graphic software VEUSZ.

2.4. Direct tensile test setup

Dog-bone specimens designed for the direct tensile test recommended by the Japan Society of Civil Engineers [16] were fabricated. These specimens had a cross-sectional area of 30 × 13 mm^2 and gauge length of 80 mm. Each specimen was installed on a universal testing machine (UTM) with a capacity of 300 kN. Two linear variable differential transformers with a capacity of 10 mm were set on both sides of the gauge length of the specimens, as shown in Fig. 2. The tensile stress (MPa) was measured by dividing the load (N) by the cross-sectional area (mm^2), and the strain (mm/mm) was measured by dividing the average displacement (mm) by the gauge length (mm). The loading rate was fixed at 0.4 mm/min.

2.5. Evaluation of interfacial shear stress

This test was conducted to compare the results of the single-fiber pullout experiments on fibers subjected to the same chemical treatment method. A specimen in which the fibers were embedded in separate UHPC at an inclination angle of 45° was employed in the single-fiber pullout test. An understanding of the fibers' independent behavior within UHPC is advantageous for this test; nevertheless, an understanding of the tensile behavior of composites is crucial because its behavior is often contrary to the single fiber pullout behavior [6]. The test setup for the single-fiber pullout behavior has been detailed in an existing study [17]. In particular, studies [18, 19] report that the fiber distribution inside a composite is not uniform. Instead, Yoo et al. [20] suggested a probability density function for fiber orientation distributions. The probability of the fibers being oriented at an inclination of 30–45° was the highest among all the orientations. Therefore, the results of previous experiments on fibers embedded at an inclination of 45° [15] were mainly cited and compared with the direct tensile test results. The pullout load measured from the load cell can be transferred to the shear stress using Eq. (2).

$$\tau(s) = \frac{P(s)}{\pi d_f (L_E - s)} \tag{2}$$

where $\tau(s)$ and $P(s)$ denote the shear stress and pullout load at a certain slip, respectively, d_f depicts the fiber diameter, and L_E represents the initial embedment length.

3. Experimental results and discussion

3.1. Examination of surface morphologies of chemically treated steel fibers

The surface morphology of each fiber, imaged using AFM, is shown in Fig. 3. Notably, no foreign substances were observed on the surface of the plain fiber, and its roughness parameter, R_q, was the lowest among all the samples (38.7 nm). In the case of acetone washing, the surface roughness increased slightly after the stainless-steel surface was cleaned [10]. Nevertheless, the AFM image appears quite smooth, such that any differences with the image of the untreated fiber are not distinguishable by the naked eye. The few swells observed on the surface might have occurred during the storage and transfer stages before being photographed and after being washed. In addition, its roughness parameter, R_q, was low (55.9 nm), i.e., the second lowest roughness after that of the plain fiber. Because the solution utilized for acid washing was of considerable strength (hydrochloric acid solution with a concentration of 35%), it not only caused hydrogen embrittlement on the coating and ferrite formation on the fiber surface, but it also dissolved the fiber. Following this reaction, the surface roughness increased, and its R_q increased significantly, resulting in the highest roughness value among all the treatment methods, with the exception of that for EDTA chelation (151.5 nm). Zinc phosphating is a coating method that is used to form Zn-based crystals on the surface; this method results in an enhanced surface roughness [21]. As demonstrated in the scanning electron microscopy (SEM) images reported in a study [15], zinc phosphating creates a groove in the axial direction, which can be confirmed from the AFM image (refer to Fig. 3). Long grooves were formed at regular intervals, and as a result, the R_q increased to 97.7 nm. The silica coating allowed small SiO_2 particles to form over the entire fiber surface. The diameter of the coated SiO_2 particles varied from 0 to 10 μm; consequently, the surface roughness was revealed to be 87.2 nm, which is a value 2.25 times greater than that of the plain fiber. The compositions of these particles were identified through energy-dispersive spectroscopy (EDS) [15]; SiO_2 particles actively produce calcium silicate hydrates (C-S-H) with cement in fresh UHPC hydrates, effectively lowering the porosity around the fibers. According to the test results, EDTA chelation was the most effective method for increasing the surface roughness. For immersion times of 6, 12, and 18 h, the roughness increased significantly to 5.1, 17.1, and 20.5 times, respectively, owing to the chelating effect. Chelating refers to the process in which the EDTA captures ionized ferrite and the combination of EDTA and Fe^{2+} flows out into the solution. Because the internal structure of a steel fiber comprises a cluster of fibrils owing to the cold-drawn manufacturing process, the fibrils peel off individually during this process. This phenomenon is prominent in the SEM image reported by Chun et al. [15], and it can also be confirmed through the AFM images. Numerous furrows that formed along the axial direction of the fiber were detected on the fiber surface, and the depth and width of the furrows increased considerably as the immersion time increased.

3.2. Tensile stress versus strain curves

The tensile behavior of UHPC is the result of a series of processes, as follows: In the initial stage, the first crack occurred when the load exceeded the tensile strength of the matrix. As the tensile load increased, the fibers that were distributed along the crack surface exhibited a fiber-bridging effect. When the external load exceeded the bond strength between the fiber and the matrix, the fibers partially debonded. At this stage, multiple cracks occurred because the increased bridging force of the fibers exceeded the tensile strength of the matrix in other areas. This mechanism is different from that of the single cracking of the fiberless UHPC, and this process can absorb a large amount of energy before the emergence of crack localization owing to its strain-hardening behavior.

The experimentally obtained tensile stress–strain curves are plotted in Fig. 4. Acetone washing resulted in the most ideal curve compared to the other treatment methods, including EDTA chelation. The curve for acetone washing is located above all the other curves; it indicates a remarkable strain-hardening behavior with a strain capacity of approximately 0.8%. This result is consistent with that of the higher shear strength at the fiber/matrix interface, as shown in Fig. 5, which was achieved when the steel fiber was treated with acetone washing.

Acid washing and zinc phosphating resulted in strain-hardening behavior as well, but the strain capacities remained at 0.63% and 0.47%, respectively, at which crack localization occurred earlier. Although the initial tensile stress increased rapidly, the hardening section was shortened, which seems to be caused by a decrease in shear stress after full debonding as shown in Fig. 5. The post-cracking stiffness of UHPC was higher for steel fibers treated by acid washing and zinc phosphating compared to the plain steel fibers, leading to lower tensile strain capacities.

Considering the pullout test results [15], silica coating was deemed a remarkable treatment method that yielded satisfactory performance in the direct tensile test, unlike that of the single fiber pullout test, wherein the fiber broke owing to an excessively high bond strength. This breakage was attributed to the essential matrix volume per fiber. As reported in studies [22,23], a certain matrix volume must be ensured for the fiber bridging effect and for appropriate pullout without breakage. Kim et al. [24] investigated the matrix volume effect based on the spacing between the fibers embedded in UHPC. In a single fiber pullout experiment, wherein each fiber had a UHPC matrix volume of $25 \times 25 \times 30$ mm^3 or more, the fiber broke when the bond stress exceeded the tensile strength of the fiber: the matrix firmly held the fibers together with sufficient density and stiffness. However, in the direct tensile test, the fibers were pulled out with relative ease, exhibiting strain-hardening behavior with appropriate shear stress. As the fibers were pulled out, frictional shear stress was generated owing to the roughened surface of the silica-coated fibers ($R_q = 87.2$ nm); thus, the tensile resistance performance was exerted for a long period, resulting in the highest strain capacity of 1.22% among all the UHPC samples.

The stress–strain curve according to the EDTA treatment time was in agreement with the shear stress and normalized slip behaviors of the steel fibers in the UHPC matrix. The results of the pullout test indicated slip-softening behavior with an increase in the immersion time; the strain capacity of the tensile specimen continuously decreased from 0.90% at 0 h (plain) to 0.56% at 18 h. Evidently, the UHPC samples reinforced with steel fibers treated for 6 h exhibited better tensile performance than the plain fiber sample owing to the appropriately modified fiber surface. Owing to the chelating effect of the EDTA electrolyte solution, the surface of the steel fiber was considerably rougher than before, which led to an increased fiber/matrix bonding area and frictional resistance. However, steel fibers treated for extended periods (12 and 18 h) in the EDTA electrolyte solution exhibited lower shear strengths at the fiber/matrix interface than the plain fibers and those treated for 6 h in the same UHPC matrix. This reduced shear strength may result from the (1) excessive stress concentration at the fiber exit, leading to matrix spalling [25], and (2) decreased weakened stiffness of the fiber surface [26]. Therefore, the fiber sample that was treated for 12 h exhibited a tensile behavior similar to that of the plain fiber sample owing to the advantages and disadvantages of the enhanced fiber surface roughness. The tensile stress–strain curve of the fiber samples treated for 18 h did not indicate an appropriate bridging effect owing to the reduced stiffness along the fiber cross-section; the performance deteriorated significantly to the extent that strain-softening behavior was noted.

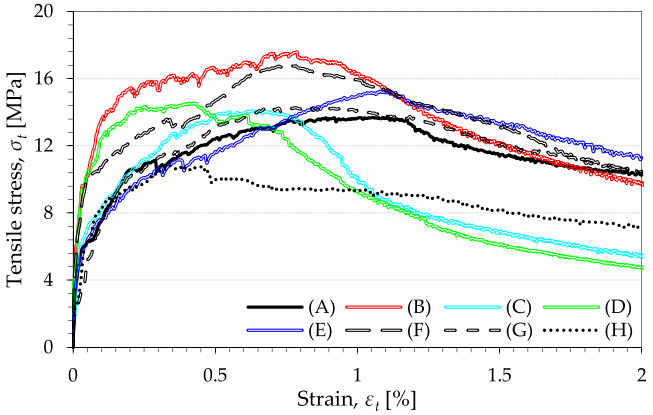

Fig. 4. Tensile stress versus strain curves.

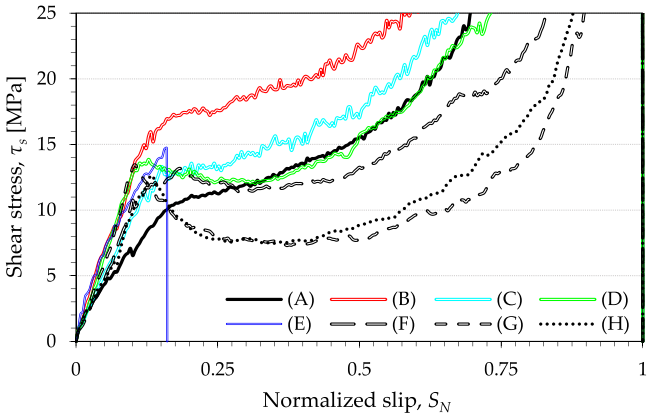

Fig. 5. Shear stress versus normalized slip curves [15].

3.3. First and post-cracking tensile strengths

The strain-hardening or strain-softening behavior of fiber-reinforced concrete (FRC) is generally evaluated according to the slope between the first cracking point and the post-cracking point on the stress–strain curve [27]. Generally, the post-cracking point is considered to be more important than the first cracking point; however, in this study, the chemical treatment method had a significant influence on the shear stress of the fiber, which was related to the first cracking strength.

Chun et al. [15] plotted the shear stress curve considering the initial chemical bonding, and the following order of the shear stress immediately before full debonding of the fiber was reported: acetone washing > zinc phosphate > acid washing > plain (the silica-coated fiber had ruptured). This result was related to that of the first cracking strength of the tensile specimen, as shown in Fig. 4. The detailed test results of the tensile parameters for all modifications are summarized in Fig. 6 and Table 2. The tensile stresses at the first and post-cracking points of the plain fiber-reinforced sample were observed to be 8.39 MPa and 14.88 MPa, while the corresponding strains were 0.10% and 0.90%, respectively. The slopes of these two points imply strain-hardening behavior in the same context as that when evaluating the degree of slip hardening.

Acetone washing resulted in strong adhesion, which was demonstrated by the effective reaction with the water in the mixture on a clean surface without impurities and afforded the highest first cracking strength of 12.17 MPa among all the treatment methods. After debonding, the tensile stress increased to a post-cracking strength of 17.76 MPa. Under acetone washing, the slope between the two points corresponded to 93% of that for the plain sample, which was similar to the slope proportion of the shear stress after debonding.

Acid-washed fibers cannot effectively adapt to tensile forces along directions other than the axial direction because of hydrogen embrittlement [28]. As detailed previously, the fiber arrangement in the composite is affected by the pouring method and rarely coincides with the axial direction. Thus, when the acid-washed fibers were mixed with fresh concrete before pouring, their contribution to the tensile performance was insignificant. The slope ratio of acid washing was 133%, i.e., from 8.43 to 14.22 MPa, which is sufficiently high to achieve strain-hardening behavior. The upward trend in the curve after the first crack, despite the weakening of the fibers owing to hydrogen embrittlement, is attributed to the high roughness of 114 nm, which resulted in a physical anchorage effect at the crack surface and interface.

Zinc phosphating method resulted in the most unfavorable changes. The post-cracking strength increased slightly to 15.10 MPa, whereas the strain capacity decreased to 0.47%, resulting in a considerably short hardening period: the compound crystals of zinc and calcium hydrate weakened the fiber–matrix interface [11]; therefore, sufficient shear stress could not be applied to most of the slip area of the fiber.

A slope ratio of 88%, i.e., from 7.16 to 15.36 MPa, was observed for the silica coating method; this method was expected to exert a significant effect in terms of enhancing the tensile performance; however, the tensile strength increased slightly, whereas the strain capacity increased significantly. The silica on the fiber surface filled the surrounding matrix, rendering a more compact matrix which considerably improved the frictional resistance. This combination of a compact interface and the high roughness of the fiber surface allowed the fibers to be pulled continuously; therefore, the load increased steadily.

The variations according to the immersion time in the EDTA electrolyte solution were notably similar to those in the pullout test results. For a treatment period of 6 h, the first and post-cracking tensile strengths increased to 9.44 MPa and 18.49 MPa, respectively; however, for a treatment period of 12 h, the tensile strengths deteriorated. Furthermore, for a treatment period of 18 h, the performance of the fibers was quite poor. As the EDTA electrolyte solution peels off the brass coating and ferrite of the fibers via chelation, the diameter of the fibers inevitably decreases over time. As reported in a study [14], the optimal period for EDTA treatment varies depending on the strength and properties of the matrix. For the mix proportion and steel fibers used in this study, the optimal treatment period was approximately 6 h.

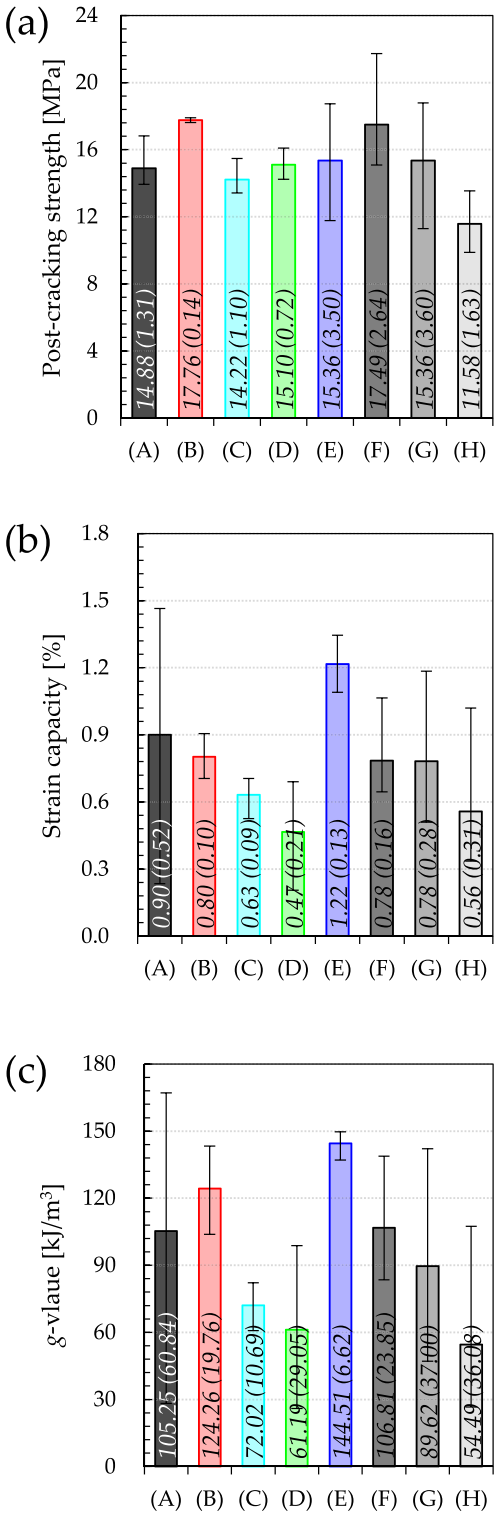

Fig. 6. Summary of tensile parameters: (a) post-cracking strength, (b) Strain capacity, and (c) *g*-value.

3.4. Energy absorption capacity

The parameter for evaluating the energy absorption capacity in direct tensile tests is the *g*-value, as suggested in a study [29]; this parameter represents the area under the stress–strain curve up to the peak. Therefore, it is complexly affected by the strain capacity and

Table 2
Summary of direct tensile test results.

Modification	Parameters					
	σ_{fc} (MPa)	ε_{fc} (%)	σ_{pc} (MPa)	ε_{pc} (%)	g-value (kJ/m^3)	R_f (nm)
Plain (EDTA chelating-0 h)	8.39 (2.45)	0.10 (0.11)	14.88 (1.31)	0.90 (0.52)	105.25 (60.84)	38.73
Acetone washing	12.17 (2.58)	0.07 (0.04)	17.76 (0.14)	0.80 (0.10)	124.26 (19.76)	55.94
Hydrochloric acid washing	8.43 (0.51)	0.10 (0.07)	14.22 (1.10)	0.63 (0.09)	72.02 (10.69)	151.47
Zinc phosphating	9.96 (1.82)	0.04 (0.02)	15.10 (0.72)	0.47 (0.21)	61.19 (29.05)	97.66
Silica coating	716 (0.74)	0.07 (0.03)	15.36 (3.50)	1.22 (0.13)	144.51 (6.62)	87.20
EDTA chelating-6 h	9.44 (1.40)	0.07 (0.05)	17.49 (2.64)	0.78 (0.16)	106.81 (23.85)	198.07
EDTA chelating-12 h	8.05 (2.50)	0.12 (0.06)	15.36 (3.60)	0.78 (0.28)	89.62 (37.00)	662.47
EDTA chelating-18 h	8.18 (1.32)	0.10 (0.05)	11.58 (1.63)	0.45 (0.31)	54.49 (36.08)	792.61

[Note] σ_{fc}= first cracking stress, ε_{fc}= first cracking strain, σ_{pc}= post cracking stress, ε_{pc}= post cracking strain, g-value = energy absorption capacity, and R_f= root mean square surface roughness, () = standard deviation

tensile strength. The g-value of the plain fiber-reinforced sample was 105.3 kJ/m^3, which is the sufficiently high to be ranked in the level 4 FRC [29]. In particular, solely the chemical treatment methods of acetone washing, silica coating, and EDTA chelation for 6 h increased the g-value by approximately 18.1%, 37.3%, and 1.5%, respectively. These three methods resulted in superior post-cracking tensile strengths and strain capacities compared to those of plain fibers; these treatment methods do not cause damage to the fibers: a feature common to these three methods. Acetone washing removes foreign substances and increases both the chemical bond strength and frictional shear stress. Moreover, the silica coating method promotes the formation of C–S–H by coating the fiber surface with SiO_2 particles, which likely improves the density within a certain volume adjacent to the surface of the fiber. Owing to the continuously generated friction resulting from the densely packed adherent hydrate particles at the fiber–matrix interfaces, the UHPC samples reinforced with silica-coated steel fibers exhibited the highest g-value of 144.51 kJ/m^3 among all the UHPC samples. The chemical treatment with EDTA electrolyte solution treatment for an optimal immersion time of approximately 6 h resulted in a notable increase in the roughness of the steel fibers. The aforementioned modifications prevented the fibers from being pulled out with relative ease and allowed them to absorb more energy under a high load that was steadily applied until the peak load value was attained.

In contrast, acid washing deteriorated the fiber structure through hydrogen embrittlement, whereas zinc phosphating weakened the fiber–matrix interface owing to the formation of compound crystals of zinc and calcium phosphate, resulting in low g-values of 72.0 and 61.2 kJ/m^3, respectively. EDTA treatment for a duration of 12 h reduced the fiber stiffness and diameter, resulting in poor tensile performance. The samples treated for 12 h exhibited a g-value of 89.6 kJ/m^3, whereas those treated for 18 h demonstrated a value of 54.5 kJ/m^3, which implies that an extended period of treatment with the EDTA electrolyte solution (specifically, treatments exceeding 6 h) negatively influence the energy absorption capacity of the ultra-high-performance fiber-reinforced concrete (UHPFRC).

4. Conclusion

In this study, the direct tensile behaviors of UHPC reinforced with plain and chemically modified steel fibers were investigated. The surface morphologies of these fibers were analyzed through their AFM images, and their tensile parameters such as the post-cracking strength, strain capacity, and g-value were calculated. Considering the probable fiber orientations, the interfacial shear stress results obtained from the 45°-inclined fiber pullout experiments were compared; on the basis of these test results, the following conclusions were drawn:

1) Acetone washing was the most effective method for increasing the post-cracking tensile strength of the UHPFRC. The cleansing effect of acetone improved the bonding between the fiber and the matrix, resulting in a tensile strength that was 19.3% greater than that of the control specimen.
2) The maximum strain capacity and g-value were observed for the nanosilica-coated fibers: 1.22% and 144.51 kJ/m^3, respectively. The dense interfacial zone and compacted fibers enhanced the shear stress, leading to an outstanding strain-hardening behavior.
3) The optimal immersion time for the EDTA electrolyte solution treatment was 6 h, which improved the tensile strength by 17.5%. In contrast, a longer immersion duration of 18 h reduced the fiber stiffness and diameter, resulting in deterioration of the tensile performance. The strain capacity and the g-value decreased by 37.8% and 48.2%, respectively: the performance of this treatment method the poorest among all methods.
4) Acid washing and zinc phosphating increased the surface roughness of the fibers; nevertheless, the enhanced surface roughness did not improve the tensile performance. Furthermore, these treatment methods are not viable for composites: the corresponding strain capacity and g-value were drastically reduced by a value greater than 30%.
5) The tensile behavior of UHPFRC that was subjected to chemical treatment of fibers is correlated with the shear stress in the pullout behavior of the 45°-inclined fibers. The higher the shear stress after debonding of the single fiber, the more desirable will be the strain-hardening behavior of the composite.

Declaration of Competing Interest

The authors declare that they have no known competing financial interests or personal relationships that could have appeared to influence the work reported in this paper.

Acknowledgements

This work was supported by the National Research Foundation of Korea (NRF) grant funded by the Korea government (MSIT) (No. 2021R1A2C4001503).

References

[1] M. Xu, B. Hallinan, K. Wille, Effect of loading rates on pullout behavior of high strength steel fibers embedded in ultra-high performance concrete, Cem. Concr. Compos. 70 (2016) 98–109, https://doi.org/10.1016/j.cemconcomp.2016.03.014.
[2] K. Wille, D.J. Kim, A.E. Naaman, Strain-hardening UHP-FRC with low fiber contents, Mater. Struct. Constr. 44 (2011) 583–598, https://doi.org/10.1617/s11527-010-9650-4.
[3] K. Wille, A.E. Naaman, Pullout behavior of high-strength steel fibers embedded in ultra-high-performance concrete, Acids Mater. J. 109 (2012) 479–488, https://doi.org/10.14359/51683923.
[4] D.Y. Yoo, N. Banthia, Size-dependent impact resistance of ultra-high-performance fiber-reinforced concrete beams, Constr. Build. Mater. 142 (2017) 363–375, https://doi.org/10.1016/j.conbuildmat.2017.03.080.
[5] A. Le Hoang, E. Fehling, Influence of steel fiber content and aspect ratio on the uniaxial tensile and compressive behavior of ultra high performance concrete, Constr. Build. Mater. 153 (2017) 790–806, https://doi.org/10.1016/j.conbuildmat.2017.07.130.
[6] B. Chun, D.Y. Yoo, Hybrid effect of macro and micro steel fibers on the pullout and tensile behaviors of ultra-high-performance concrete, Compos. Part B Eng. (2019) 344–360, https://doi.org/10.1016/j.compositesb.2018.11.026.
[7] D.Y. Yoo, S. Kim, G.J. Park, J.J. Park, S.W. Kim, Effects of fiber shape, aspect ratio, and volume fraction on flexural behavior of ultra-high-performance fiber-reinforced cement composites, Compos. Struct. 174 (2017) 375–388, https://doi.org/10.1016/j.compstruct.2017.04.069.
[8] T. Stengel, Effect of surface roughness on the steel fibre bonding in ultra high performance concrete (UHPC), Nanotechnol. Constr. 3 (2009) 371–376, https://doi.org/10.1007/978-3-642-00980-8_50.
[9] B. Chun, D.Y. Yoo, N. Banthia, Achieving slip-hardening behavior of sanded straight steel fibers in ultra-high-performance concrete, Cem. Concr. Compos. 113 (2020), 103669, https://doi.org/10.1016/j.cemconcomp.2020.103669.
[10] X. Fu, D.D.L. Chung, Bond strength and contact electrical resistivity between cement and stainless steel fiber: their correlation and dependence on fiber surface treatment and curing age, Acids Mater. J. 94 (1997) 203–208.
[11] T. Sugama, N. Carciello, L.E. Kukacka, G. Gray, Interface between zinc phosphate-deposited steel fibres and cement paste, J. Mater. Sci. 27 (1992) 2863–2872, https://doi.org/10.1007/BF01154093.
[12] Z. Pi, H. Xiao, J. Du, M. Liu, H. Li, Interfacial microstructure and bond strength of nano-SiO2-coated steel fibers in cement matrix, Cem. Concr. Compos. 103 (2019) 1–10, https://doi.org/10.1016/j.cemconcomp.2019.04.025.
[13] Z. Pi, H. Xiao, R. Liu, M. Liu, H. Li, Effects of brass coating and nano-SiO2 coating on steel fiber–matrix interfacial properties of cement-based composite, Compos. Part B Eng. 189 (2020), 107904, https://doi.org/10.1016/j.compositesb.2020.107904.
[14] S. Kim, S. Choi, D.Y. Yoo, Surface modification of steel fibers using chemical solutions and their pullout behaviors from ultra-high-performance concrete, J. Build. Eng. 32 (2020), https://doi.org/10.1016/j.jobe.2020.101709.
[15] B. Chun, S. Kim, D.Y. Yoo, Benefits of chemically treated steel fibers on enhancing the interfacial bond strength from ultra-high-performance concrete, Constr. Build. Mater. 294 (2021), 123519, https://doi.org/10.1016/j.conbuildmat.2021.123519.
[16] JSCE, Recommendations for design and construction of ultra high performance fiber reinforced 19 concrete structures (Draft), Japan Soc. Civ. Eng. (2004).
[17] D.-Y. Yoo, B. Chun, Enhancing the rate dependent fiber/matrix interfacial resistance of ultra-high-performance cement composites through surface abrasion, J. Mater. Res. Technol. 9 (2020), https://doi.org/10.1016/j.jmrt.2020.06.080.
[18] H. Huang, X. Gao, L. Li, H. Wang, Improvement effect of steel fiber orientation control on mechanical performance of UHPC, Constr. Build. Mater. 188 (2018) 709–721, https://doi.org/10.1016/j.conbuildmat.2018.08.146.
[19] M. Roy, C. Hollmann, K. Wille, Influence of volume fraction and orientation of fibers on the pullout behavior of reinforcement bar embedded in ultra high performance concrete, Constr. Build. Mater. 146 (2017) 582–593, https://doi.org/10.1016/j.conbuildmat.2017.04.081.
[20] D.Y. Yoo, S.T. Kang, Y.S. Yoon, Effect of fiber length and placement method on flexural behavior, tension-softening curve, and fiber distribution characteristics of UHPFRC, Constr. Build. Mater. 64 (2014) 67–81, https://doi.org/10.1016/j.conbuildmat.2014.04.007.
[21] S. Riahi, A. Nemati, A.R. Khodabandeh, S. Baghshahi, Investigation of interfacial and mechanical properties of alumina-coated steel fiber reinforced geopolymer composites, Constr. Build. Mater. 288 (2021), 123118, https://doi.org/10.1016/j.conbuildmat.2021.123118.
[22] L. Flanders, T. Rushing, L. Landis, Energy dissipation mechanisms in the fracture of fiber reinforced ultra high performance concrete, in: 4th International Symposium on Ultra-High Performance Concrete High Performance Construction Materials (2016) 1–8.
[23] D.Y. Yoo, Y.S. Jang, B. Chun, S. Kim, Chelate effect on fiber surface morphology and its benefits on pullout and tensile behaviors of ultra-high-performance concrete, Cem. Concr. Compos. 115 (2021), 103864, https://doi.org/10.1016/j.cemconcomp.2020.103864.
[24] D.Y. Yoo, J.J. Kim, J.J. Park, Effect of fiber spacing on dynamic pullout behavior of multiple straight steel fibers in ultra-high-performance concrete, Constr. Build. Mater. 210 (2019) 461–472, https://doi.org/10.1016/j.conbuildmat.2019.03.171.
[25] P.A. Krahl, G. de Miranda Saleme Gidrão, R.B. Neto, R. Carrazedo, Effect of curing age on pullout behavior of aligned and inclined steel fibers embedded in UHPFRC, Constr. Build. Mater. 266 (2021), 121188, https://doi.org/10.1016/j.conbuildmat.2020.121188.
[26] M. Amran, R. Fediuk, H.S. Abdelgader, G. Murali, T. Ozbakkaloglu, Y.H. Lee, Y.Y. Lee, Fiber-reinforced alkali-activated concrete: a review, J. Build. Eng. 45 (2022), 103638, https://doi.org/10.1016/j.jobe.2021.103638.
[27] C. Redon, V.C. Li, C. Wu, H. Hoshiro, T. Saito, A. Ogawa, Measuring and modifying interface properties of PVA fibers in ECC matrix, J. Mater. Civ. Eng. 13 (2001) 399–406.
[28] M.R. Louthan, Hydrogen embrittlement of metals, Mater. Sci. Eng. 10 (1972) 357–368, https://doi.org/10.1016/0025-5416(72)90109-7.
[29] K. Wille, S. El-Tawil, A.E. Naaman, Properties of strain hardening ultra high performance fiber reinforced concrete (UHP-FRC) under direct tensile loading, Cem. Concr. Compos. 48 (2014) 53–66, https://doi.org/10.1016/j.cemconcomp.2013.12.015.